Sustainable solid-state method of synthesis, characterisation, and photoluminescence studies of Yb^{3+}/Ho^{3+} doped YPO_4 nanomaterials

Sirisha Bandi[1,2*], *Phani* Raja Kanuparthy[2], *Venkata* Nagendra Kumar Putta[2], *Kusuma* Ashok Kumar[1] and *Saroja* Rani Bhupatiraju[3]

[1]B V Raju Institute of Technology, Narsapur, Telangana, India.
[2]Department of Chemistry, GITAM deemed to be University, Hyderabad, Telangana, India.
[3]Gokaraju Rangaraju Institute of Engineering and Technology, Hyderabad, Telangana, India.

Abstract. To encourage the production of $[PO_4]^{3-}$ groups, a group of up-converting &down-converting YPO_4 Yttrium phosphate compounds were synthesized using the solid-state technique in a basic environment. The noble pureness of the doped matrix was confirmed by the structural studies and Rietveld analysis, whereas growth in the part of the YPO_4: Yb, Ho structures was discovered with a higher dopant concentration. The phosphates group, along with the ions Yb^{3+} and Ho^{3+}, allowed for the UC&DC luminescence. While we observe up-conversion luminescence with colour under the 980 nm continuous movement of wave laser irradiation had been set on the way to the red area, the powerful green emission had been produced by 300 nm excitation. Following the results, materials that are resistant to different applications can use synthetic phosphors.

Keywords: dual-mode luminescence, up-conversion(UC), down-conversion(DC), Yttrium ion, Ytterbium ion, Holmium ion, charge transfer(CT)

1 Introduction

Today, trivalent lanthanide ions stay broadly employed in inorganic luminous materials for varied applications, together with lasers, drug delivery, bio-imaging, light emitting diodes, and counterfeit detection [1], [2], [3], [4], and [5]. The phosphor must be chemically and thermally stable in the last two applications due to the additional processing, placement in the appropriate medium (paper or polymer), and operating temperatures of the finished product. Anti-counterfeiting phosphors are created to have unique, hard-to-replicate properties that increase their efficacy in anti-counterfeiting applications [6]. The high colour tunability of phosphors that show dual-mode emission, and intense under stimulation in both the UV and near-infrared (NIR), makes them ideal for anti-counterfeiting reasons. Yttrium ion: Y^{3+} Chemical element yttrium is frequently added to phosphors as a dopant to increase their luminous qualities. Yttrium phosphate (YPO_4) is a unique kind of phosphor that

* Corresponding Author: sireesha.b@bvrit.ac.in

comprises ions from both gadolinium and phosphate. Yb^{3+}: The Ytterbium Ion Another chemical used as a dopant in phosphors is ytterbium [7].

Holmium ion, Ho^{3+} (The chemical element holmium is employed in phosphors as a dopant.) Phosphate ion $[PO_4]^{3}$- (The anion phosphate is made up of phosphorus and oxygen atoms. It is a crucial element in phosphors made of phosphate). A material emits light when it absorbs energy and then releases it as light, a process known as luminescence. The term "dual-mode" describes a phosphor's capacity to exhibit luminescence under two distinct wavelengths. i.e the UV (= 300 nm) excitation was used to produce the strong green emission, while the N-IR (= 980 nm) was used to produce the red up-conversion luminescence. Which proposed many anti-counterfeiting luminous constituents built on Ln(III) ions. In their review [8]. Conversely, because of dual-mode and adjustable emission, the YPO_4 doped with Yb^{3+}& Ho^{3+} ions described here outperforms other systems [9], [10].

Its excitation type result from a well-matched matrix structure and a appropriate mix of Y^{3+} dopant ions. As a result, we may use UV light to stimulate the phosphate medium & witness its broad and strong emission. NIR excitation, on the other hand, causes the usual Y^{3+} emission with crisp and well-defined bands. The colour of the illumination changes dramatically in both circumstances. Furthermore, their crystal structure allows for P-O charge transfer, allowing for powerful broadband illumination emitting through their host [11], [12], [13]. According to research, the alkali metal phosphates of nanophosphors have strong white photoluminescence, and the colour can be changed by the insertion of Y^{3+} enhancing alkali cations in the structure. Feature indicates that materials are ideally suited for W-LED solicitations [14, 15], [16], [17], [18], and [19]. So far, solid-state methods have been used to create phosphate nanophosphors.

This process necessitates high-temperature calcination, which increases grain size. Even in solid-state settings, YPO_4 production requires microstructure or the presence of surfactants to produce nanoparticles [19], [20]. Since there is a difficult phosphate structure, incorporating Y^{3+} dopants at greater quantities is problematic consequently, the Stokes process has been examined in such systems. As a result, the up-converting & down-converting phosphate structure must be created and studied. The YPO_4 structure doped with Yb & Ho ions was created using a solid-state procedure in this article [21]. This composition enables the observation of visible light under stimulation in the uv and closer infrared, this is recognized as dual-mode emission.

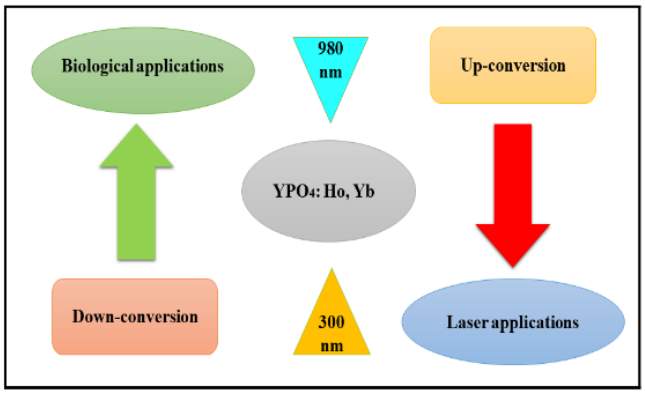

Fig. 1. Graphical representation of YPO_4:Ho^{3+}/Yb^{3+} Nanophosphors respectively.

2 Materials and Method

2.1 Chemicals and Synthesis Method

Reactants were very pure analytical grade chemicals from Sigma-Aldrich. [$Y(Ac)_3.XH_2O$], [$(NH_4)_2HPO_4$], HCl, [$(Ho(Ac)_3).XH_2O$], [$Yb(Ac)_3.XH_2O$], EG, NaOH, and H_2O Acetone are used as precursors.

2.2 Synthesis of YPO4: Ho3+/Yb3+ Nanoparticles

2.2.1 Solid-state Technique

For the sample's preparation, the solid-state procedure is used from Fig. 1. The subsequent list of the samples was generated: YPO_4:Ho^{3+} and Yb^{3+} brilliant nanoparticles are doped with 1% and 20% of Ho^{3+} and Yb^{3+}, correspondingly. A solid-state process was used to generate this product. In a classic synthesis, 5 ml of concentrated HCl fallowed by 1.46 gm of $(CH_3CO_2)_3Y.XH_2O$, 17.4 mg of $(CH_3CO_2)_3Ho.XH_2O$, and 356.96 mg of $(CH_3CO_2)_3$ $Yb.XH_2O$, 596.56mg of $(NH_4)_2HPO_4$,20ml ethylene glycol, and 5.28 gm of NaOH were added. After that, the compound are grind in the motor for at least 3 hours by adding acetone to exclude any leftover HCl. After 2-3hours of continuous grinding keep the samples for heating in further furnace at 1150^0C at for least 4-5 hours, and then we got the expected material to be formed.In the same way, secure amounts of Yb^{3+} (10@%) and Ho^{3+} (3, 5, and 7 @%), are synthesized.

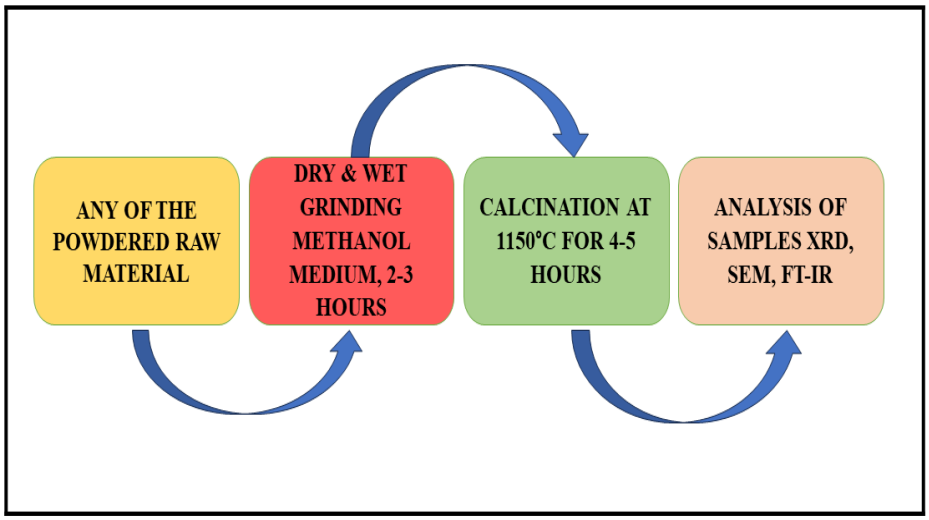

Fig. 2. Solid state method of preparation of YPO_4:Ho^{3+}/Yb^{3+} Nanophosphors.

3 Results and Discussion

3.1 XRD Sample Study

Nano phosphors YPO_4: 1at. % Ho^{3+} and 20 at. % Yb^{3+} co-doped YPO_4 is shown in Fig. 2, XRD form. These materials can be annealed at 1150 °C. A robust,and sharp of diffraction

pattern peaks shows a continuous phase with the normal monoclinic phase. at 25 degrees (2 Theta) and 35 degrees (2 Theta) and we can observe the indices i.e.(1 0 1)(2 0 0)(1 1 2)(2 1 1)(3 0 1)(3 1 2)(4 0 0). Due to impurity peaks' nonappearance , dopants are expected to be distributed all over the host lattice. Two of the greatest intensity peaks in the XRD pattern and most significant intensity peaks are observed. Diffraction patterns are closely matched with the monoclinic structure of YPO_4:Ho/Yb. JCPDS No:11- 0254 and, JCPDS No:76-1649 are matched[24]. Based on CN 8, Yb^{3+} and Ho^{3+} ions were replaced at Y^{3+} sites of the YPO_4 lattice. Since they have comparable ionic radii.

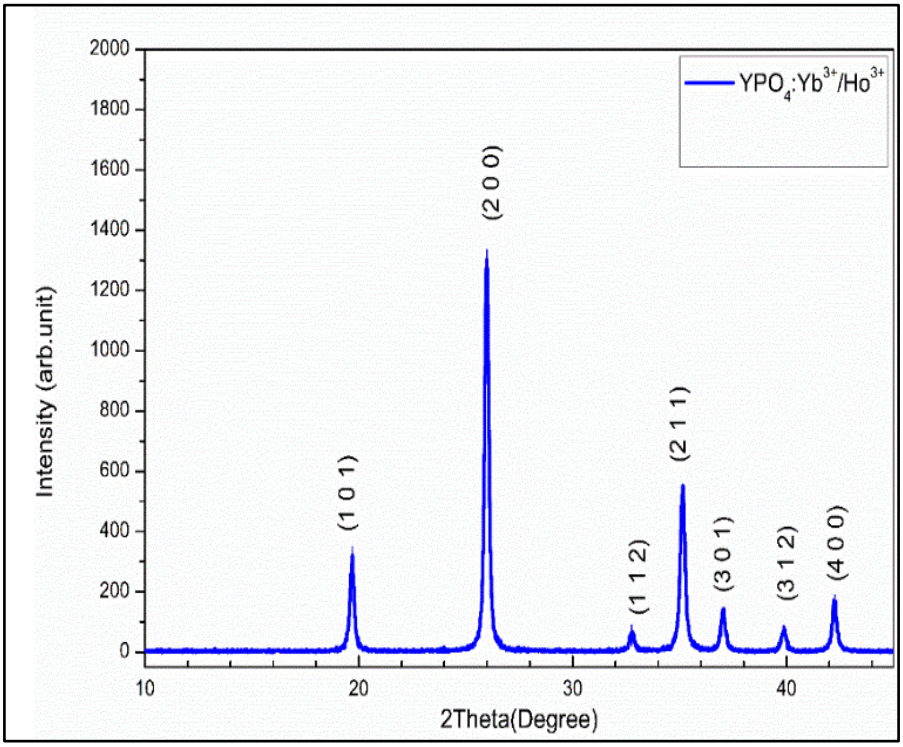

Fig. 3. XRD pattern of YPO_4:Ho^{3+}/Yb^{3+} samples**.**

3.2 SEM Study

A YPO_4:Ho^{3+}/Yb^{3+} nanophosphor material was produced and annealed at 1150 °C in the present work. An images of the nanophosphor taken using scanning electron microscopy (SEM) is shown in Fig. 3, According to the SEM picture, the nanoparticles have uneven shapes, with a sizable amount having a sponge-like appearance. In addition, certain nanoparticles with diameters ranging from a few nm have a cone-like and spherical shape. These atypical shapes and differences in particle morphology show that the conventional spherical shape with 80 nm generated from the synthesis process is not predominant in this instance.

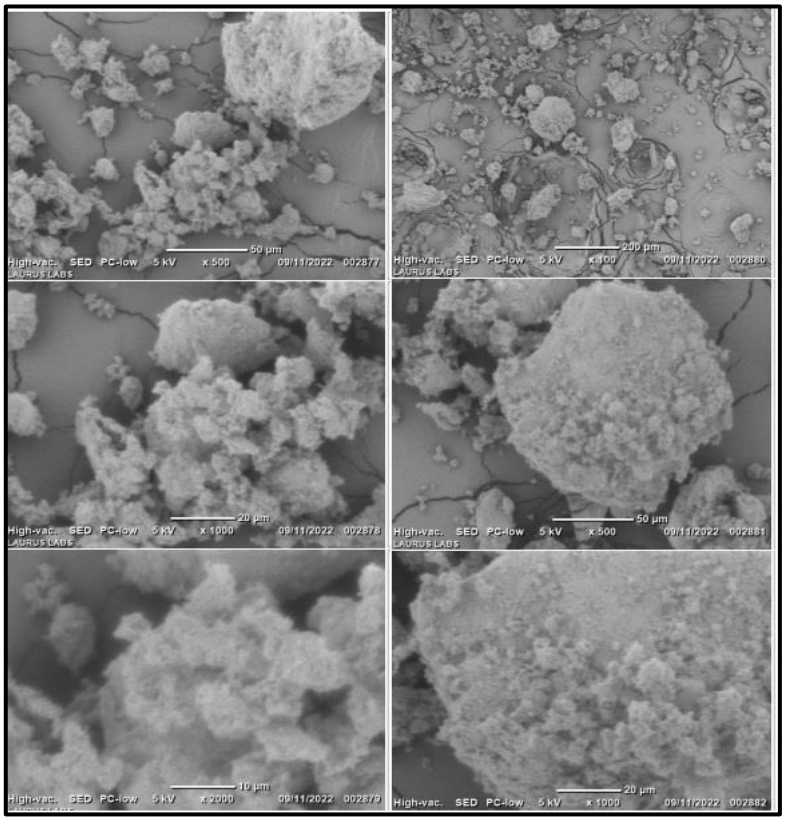

Fig. 4. SEM pattern of YPO_4:Ho^{3+}/Yb^{3+} samples respectively.

3.3 FT-IR Analysis

The vibrational structure of a produced materials was investigated using FTIR Spectroscopy with 1 cm^{-1} resolution. (Bomemn MB 102 spectrophotometer). Fig. 4, shows PO_4^{3-} peak observed at 983 cm^{-1} & 1067 cm^{-1} at 1617cm^{-1} the peak shows N-H bond, 2112 cm^{-1} peak shows base metal bonded with dopants & 3501 cm^{-1} shows O-H bond.

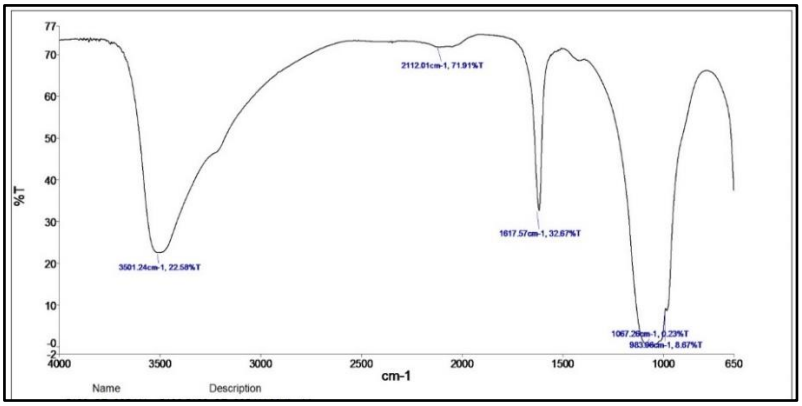

Fig. 5. FTIR pattern of YPO_4:Ho^{3+}/Yb^{3+} samples respectively

3.4 PL Spectral properties

Based on the observed host structure, the lattice incorporates a $[PO_4]^{3-}$ heterodimer with twist Td symmetry, or two $[PO_4]^{3-}$ entities sharing a corner. As a result, both the PO_4^{3-} 3d orbital and the O^{2-} 2d orbital take part in charge of electrons transference interpretation, resulting in photoluminescence. MO of $[PO_4]^{3-}$ is defined by $^1A_1$ GS and $^1T_1$ and $^3T_1$ excited states throughout this process [17],[22]. The undoped YPO_4 system exhibits a broad $^1A_1 \rightarrow {}^1T_1$ excitation band at 300 nm [17] , after doping which leads to a monoclinic structure a robust and wide emission band in the green region (525nm) are observed. Many light constituents founded. Ln (III) ions were developed aimed at anti-counterfeiting purposes. Only Ho^{3+} responds to UV irradiation, therefore several energy slopes associated with Ho^{3+} transitions: $^3D_3 \rightarrow {}^5I_5$ (455 nm), $^5F_3 \rightarrow {}^5I_8$ (525 nm), and $^5S_2, {}^5F_4 \rightarrow {}^5I_8$ (546 nm) .

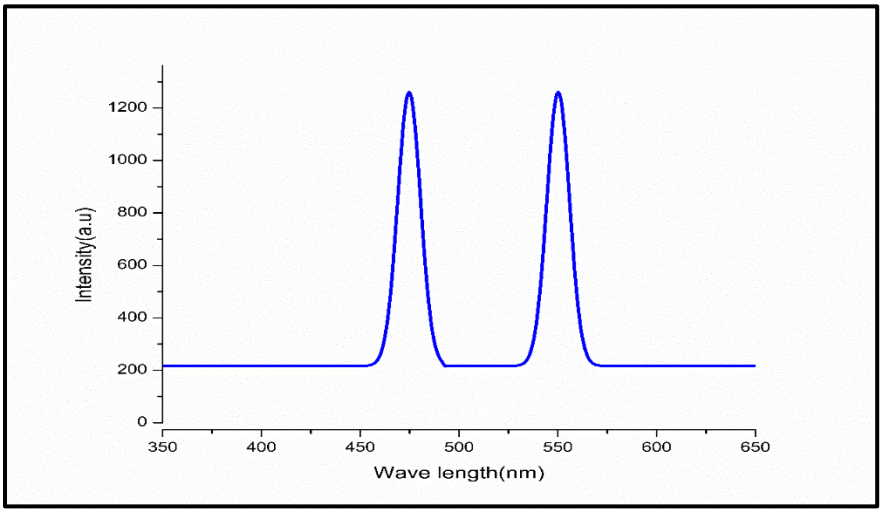

Fig. 6. PL of YPO_4: Yb, Ho Nanomaterials.

When dopants (Yb^{3+}, Ho^{3+}) were introduced, the form and magnitude of this emission band altered a little (Fig. 5, Furthermore, when its concentration rises so does the strength of specific transitions due to better energy transfer between P-O and Ho^{3+} [23]. However, the sample containing 3% Yb^{3+} and 0.5% Ho^{3+} had the highest luminescence brightness owing to geometric congruence with the YPO_4 pattern and the absence of nearby phosphate phases, which might decrease luminescence.

3.5 Upconversion luminescence

The synthetic YPO_4 samples, which have the following formula: YPO_4: x% Yb^{3+}(20%, y% Ho^{3+} engage NIR light, allowing the UC emission to be seen yet 980 nm CW excitation (Fig. 6, Most of the Yb^{3+} ion experiences $^2F_{7/2}$, $^2F_{5/2}$ excitation as a result of absorbing the 980 nm light, following the electronic structure of the dopants. Then, energy is directed towards Ho^{3+}, which is excited at the $^5I_6$ level. Ho^{3+} is in the $^5F_4$, $^5S_2$ state after absorbing one more photon and having its handover to the emitter. Several emission activities, begin immediately, including the production of green light Light at 545 nm in the $^5F_4$, $^5S_2$, to $^5I_8$ transition range.[23] At the same time, a non-radiative transition to $^5F_5$ occurs, leading to deactivation to the ground state, which is seen in the spectrum as a 656 nm emission band. One more continuing process is $^5F_4$, $^5S_2$, and $^5I_7$ deactivation-related light at 754 nm.

For several reasons, the series' changing red-to-green band intensity ratio can be attributed to colour tunability.The YPO_4: Yb, Ho structures chromaticity is tweaked towards red with a rise in the amount of Yb^{3+} and consequently higher Yb/Ho ratio due to a higher likelihood of the non-radiative $^5F_4$, $^5S_2$ $^5F_5$ deactivation. Additionally, due to the reduction in the distance between Ln^{3+} during the doping process, more interactions between these species are seen. Energy back transfers (EBT), which are characterized by (Ho^{3+}) $^5S_2$, $^5F_4$(Yb^{3+}) $^2F_{7/2}$ (Ho^{3+}) $^5I_6$ (Yb^{3+}) $^2F_{5/2}$ and (Ho^{3+}) $^5F_5$(Yb^{3+}) $^2F_{7/2}$ (Ho^{3+}) $^5I_7$, reduce the intensity of green emissions occurring at the $^5F_4$, $^5S_2$ level [24][25].

It should be observed that the Yb/Ho ratio in YPO_4 varies as the Yb^{3+} concentration rises during the series and is regularly incorporated into YPO_4 can observe the monoclinic phase. The fluctuation in the relation between luminescence intensity and laser power density allowed the researchers to understand better the mechanism underlying the upconversion process.
By examining the slope of log-log graphs in nanometers, it was possible to calculate the amount of photons involved in particular transitions. This slope is consistent with two photons taking part in these transitions. However, as evidenced by its lower luminescence intensity, the emission at 754 nm is less favoured in the upconversion (UC) process. Additionally, its intensity considerably decreases in samples with increased Yb^{3+} concentrations. When continuous wave (CW) 980 nm light is used to activate Ho^{3+}-doped phosphate phosphors (with energy levels $^5F_4$, $^5S_2$, and $^5I_7$), the amount of energy that Ho^{3+} preferentially absorbs and uses decreases the emission intensity, especially in the green light spectrum. The in-question YPO_4 phosphors have X% Yb^{3+} and 0.5% Ho^{3+}. We investigated the mechanism in the experiment for three series with fixed Ho^{3+}, namely 0.1%, 0.5%, and 1%. For the transitions in the red part of the spectrum with the highest Yb/Ho ratio for the group of YPO_4: X% Yb^{3+}, 0.1% Ho^{3+} phosphors, estimated for 545 nm and 656 nm a disparity between empirically derived and theoretical values is noted[26].

The emission line with the highest intensity at 656 nm determines the color of the resulting luminescence. The non-radiative relaxation in $^5F_4$, and $^5S_2$ allows the $^5F_5$ level, which produces the red emission, to be more productively employed. This may have an impact on the raised experimentally calculated n. In this example of the 754 nm transition, a rise in Yb^{3+} concentration is also accompanied by a decrease in the n value. Energy back transfer (EBT) is more likely to happen when the lanthanide ions are packed closely in the lattice, especially when the sensitizer content approaches 6%. As a result, the intensity of emissions from energy levels $^5S_2$, $^5F_4$, and $^5I_7$ is noticeably reduced.

The likelihood of the $^5F_4$, $^5S_2$ to $^5I_8$ transition, which results in green emission, is significantly increased in the YPO_4 series with the lowest Yb/Ho ratio, such as in YPO_4: X% Yb^{3+}, 1% Ho^{3+}. This is consistent with how things should act. The energy diagram is depicted succinctly in Fig. 6, to explain the mechanisms underlying upconversion (UC). It is crucial to be aware of the many deactivation mechanisms that nanomaterials are exposed to. Since the crystal structure is defective in lanthanide-doped structures because of the high surface-to-volume ratio, the existence of luminescence deactivation centers becomes essential.

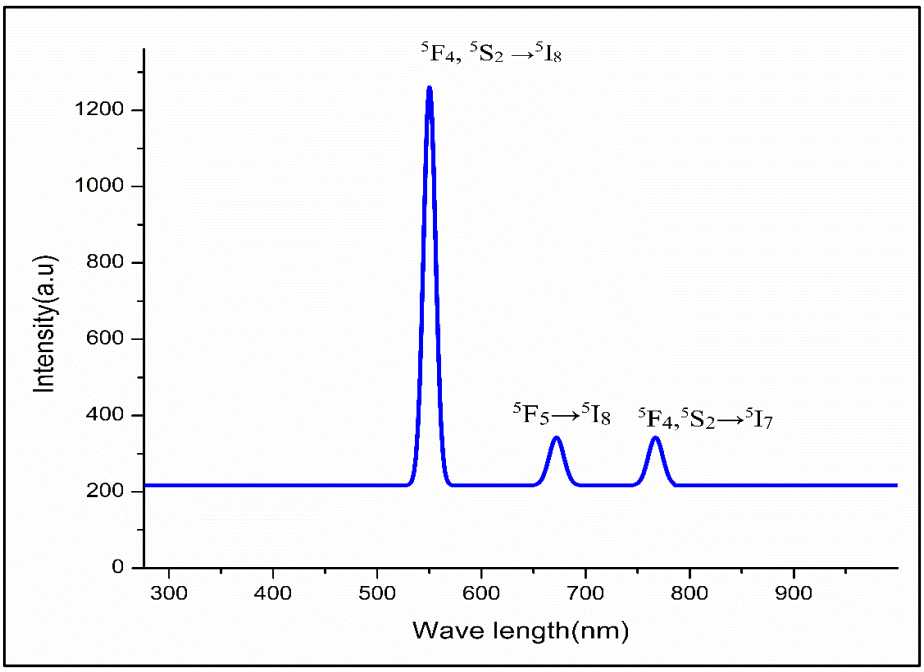

Fig. 7. Upconversion of YPO_4: Yb, Ho phosphors.

4 Conclusion

An easy solid-state technique was used in an alkaline environment to create YPO_4: Ho/Yb structures. To test the up-conversion luminescence, the structure of phosphates was doped with varied amounts of Yb^{3+} and Ho^{3+}. Structural analyses revealed that the monoclinic structure produced evidence of the YPO_4 phase when dopants were added. The preparation process is expanded to include an annealing stage. XRD research demonstrated that the synthesized nanomaterials have a propensity to aggregate. Interestingly, a specific grain's size fell inside the range.

Dual mode luminescence was demonstrated by phosphor-based phosphors, which is advantageous for anti-counterfeit applications Charge transfer inside the $[PO_4]^{3-}$ group led to green luminescence under 300 nm stimulation, and the intensity of this luminescence was enhanced for the monophasic YPO_4 complexes. Many slopes in emission spectra that correspond to different Ho^{3+} transitions in terms of ET between the host and Ho^{3+}. Additionally, the size of slopes was strongly correlated with the rise in Ho^{3+} concentration, suggesting a more efficient energy transfer. It should be observed that the dopant inclusion did not affect the colour of the photoluminescence.

Under 980 nm CW stimulation, another luminescence phenomenon emerged due to Yb^{3+}'s ability to absorb energy before transferring it to emitting Ho^{3+}sites. Present results demonstrate that as Yb^{3+} concentration rises, the luminescence colour is considerably adjusted from green to red. We can observe red emission at 656 nm, which is the brightest band in UC spectra, was created by a variety of mechanisms, including increased nonradioactive relaxation at the $^5F_4$, $^5S_2$ levels, and Yb^{3+}-Ho^{3+} (EBT). The emitted shade altered significantly during all studied samples matches most intensely for phosphors with a

low Yb: Ho ratio. Due to all of these attributes, proposed phosphors have potential applications.

5 Funding

This research received no external funding

6 Acknowledgments

Our sincere gratitude to GITAM Deemed to be University for providing research facilities.

7 Conflicts of Interest

"Here I, declare no conflict of interest." This research work (synthesis part) is completely carried out in our laboratory at GITAM Deemed to be University, Hyderabad

References

1. R.S. Perala, R. Joshi, B.P. Singh and V.N.K Putta, ACS omega. 6(30), 19471-19483 (2021).
2. R.S. Perala, B.P Singh, V.N.K Putta and R. Achary, ACS omega. 6(30), 19517-19528 (2021).
3. Y. Yu, Y. Zheng, F. Qin, L. Liu, C. Zheng and G. Chen, Optics.284(4), 1053-1056 (2011).
4. A.R. Camacho, F.J.C. Romo, A.G. Murillo and J. Oliva, Materials Letters. 226, 34-37 (2018).
5. D. Przybylska, A. Ekner Grzyb, B.F. Grześkowiak and T. Grzyb, Scientific Reports. 9(1), 8669 (2019).
6. L. Řezáčová, M. Runowski, P. Lubal, A. Szyczewski, and S. Lis, Chemical Papers. 73, 2907-2911(2019).
7. N. Kaczorowska, A. Szczeszak, W. Nowicki and S. Lis, Polyhedron. 223, 115940 (2022).
8. Y. Zhang and H. Guan, Journal of Crystal Growth. 256(1-2), 156-161 (2003).
9. Y. Fan, Z. Hu, J. Yang, C. Zhang and L. Zhu, Applied surface science. 266, 22-26 (2013).
10. K. Riwotzki, H. Meyssamy and A. Kornowski, The Journal of Physical Chemistry B.
11. S.Bandi, P. R.Kanuparthy, & V. N. K.Putta, Oriental Journal of Chemistry., 2023 ,39(4).
12. S.Bandi, P. R.Kanuparthy, & V. N. K.Putta, Asian Journal of Chemistry., 2023, 35(10).
13. C. Niu, L. Li, X. Li, Y. Lv and X. Lang, Optical Materials. 75, 68-73 (2018).
14. P. Zhao, Z. Wang, J. Chen, Y. Zhou and F. Zhang, Optical Materials. 66, 98-105 (2017).
15. G. Xu, P. Li, P. Chen, L. Cui, Z. Wang, Z. Ren and X Qin, Fuel.332, 126113 (2023).
16. Y.P. Fang, A.W. Xu, R.Q. Song, H.X. Zhang, L.P. You, J.C. Yu and H.Q. Liu, Journal of the American Chemical Society. 125 (51), 16025-16034 (2003).
17. B. Lai, L. Feng, J. Zhang, J. Wang and Q. Su, Applied Physics B. 110 ,101-110 (2013).
18. Q. Liu, W. Feng, T. Yang, T. Yi and F. Li, Nature protocols. 8(10), 2033-2044 (2013).
19. V. Kumar, P. Rani, D. Singh and S. Chawla, RSC advances. 4(68), 36101-36105(2014).
20. A. Dwivedi, E. Rai, D. Kumar, and S.-B. Rai, ACS omega. 4(4), 6903-6913(2019).

21. M. Kumar Mahata, T. Koppe, K. Kumar, H. Hofsäss and U. Vetter, Scientific Reports. 6(1), 36342 (2016).
22. T. Lyu and P. Dorenbos, Journal of Materials Chemistry C. 6(2), 369-379 (2018).
23. P. Du, X. Huang and J.S. Yu, Chemical Engineering Journal. 337, 91-100 (2018).
24. I. Földvári, A. Baraldi, R. Capelletti and N. Magnani, Optical Materials. 29(6), 688-696 (2007).
25. Y. Guan, Y. Huang, T. Tsuboi, W. Huang and C. Chen, Materials Science and Engineering: *B*. 190, 26-32 (2014).
26. N.C. Shie, W.F. Hsieh and J.T. Shy, Optics Express. 19(22), 21109-21115 (2011).